ISTITUTO NAZIONALE DI FISICA NUCLEARE

Sezione di Genova

INFN/AE-79/2
2 Agosto 1979

S. Benso and L. Rossi: A NEW METHOD FOR SUBDIVIDING CATHODES OF MULTIWIRE PROPORTIONAL CHAMBERS INTO INDEPENDENT ELEMENTS AND READING THEIR INFORMATION.

Servizio Documentazione
dei Laboratori Nazionali di Frascati

Istituto Nazionale di Fisica Nucleare
Sezione di Genova

INFN/AE-79/2
2 Agosto 1979

S. Benso and L. Rossi: A NEW METHOD FOR SUBDIVIDING CATHODES OF MULTIWIRE PROPORTIONAL CHAMBERS INTO INDEPENDENT ELEMENTS AND READING THEIR INFORMATION.

ABSTRACT.

A multiwire proportional chamber with both cathode and anode readout has been constructed and tested. A new method for subdividing the high voltage plane and reading its information is used. This allows complete flexibility in choosing the sizes and forms of the sensitive zones of the cathodes and, furthermore, makes easy the rejection of "ghost tracks" arising from high multiplicity events in the chamber.

Efficiencies for both cathodes and anodes are > 98 %, while the cross-talk between neighbouring cathodes is < 1 %. The limits of this method have been investigated with a Fourier analysis and the best combinations of the electronic parameters of such a chamber have been found.

1. - INTRODUCTION.

Different methods have already been studied for using the additional information coming from the cathodes of a multiwire proportional chamber (MWPC). Delay line[1] and charge division methods[2] give a good space resolution if sophisticated and carefully calibrated electronics is employed. Alternatively, dividing the cathode planes into individual detectors and treating them as binary elements[3] requires standard electronics but gives only rough space information. This is valuable when a low mass hodoscope is needed, particularly if a difficult shape to obtain with present scintillator techniques or operation into a magnetic field is required.

Up to now the main limitations to this detector design come from the difficulty of getting both the cathode and the anode information - thus limiting the intrinsic space accuracy of the chamber - and from the need of sacrificing part of the sensitive surface for picking up the signals.

We demonstrate that both these difficulties can be over come with the suitable use of RC filters.

2. - PROTOTYPE CHAMBER AND EXPERIMENTAL SET UP.

Our experimental set up is shown in Fig. 1.

The multiwire proportional chamber characteristics are summarized in Table I.

TABLE I

Wire spacing	2 mm
Wire diameter	20 m
Gap	3 mm
Sensitive zone	15 x 15 cm^2

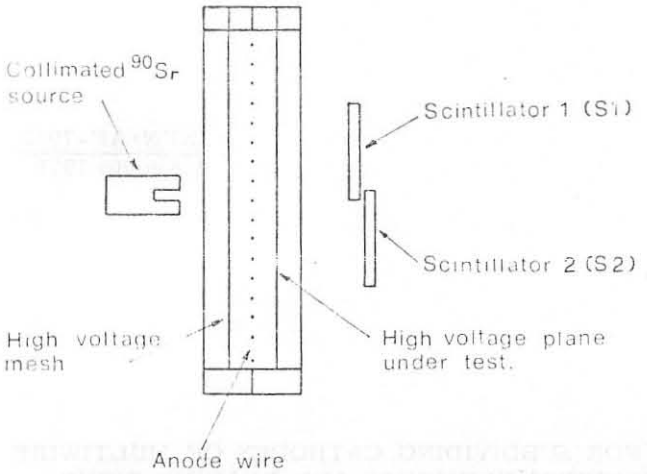

FIG. 1 - A schematic representation of the experimental set up.

The chamber was filled with a mixture of 75 % Ar, ~25 % CO_2 and a small fraction (< 1.5%) of Freon 13B1. The high voltage planes of this MWPC are shown in Fig. 2.

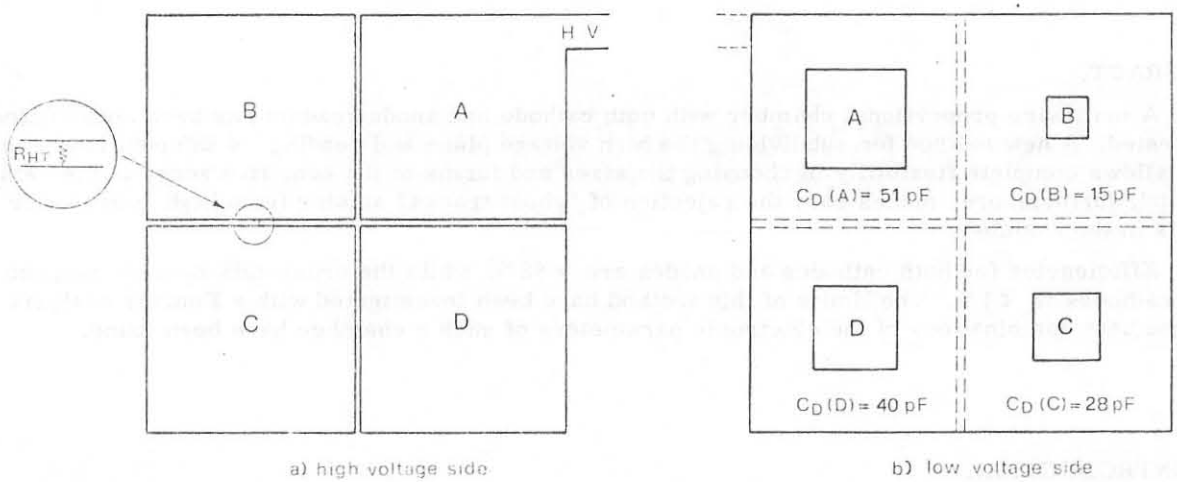

FIG. 2 - The high voltage plane of the prototype chamber. The linking resistors are obtained through graphyte deposit. a) high voltage side, b) low voltage side.

Each cathode consists of four copper squares (7.4 x 7.4 cm^2, 100 μm thick, 2 mm spaced) on a vetronite support (2 mm thick). The first receives the high voltage directly from the power supply while the others are connected in series each via a resistance $\gtrsim$ 100 KΩ obtained through a graphyte layer. The signals, induced on a cathode segment by the Townsend avalanche around a sense wire, are picked up via a high voltage capacitor made from a thin (100 μm) piece of copper glued to the reverse side of the vetronite foil. The resulting circuit is illustrated in Fig. 3.

Two aims are reached in this way : no part of the high voltage plane is devoted to transmitting the signals outside the detector, and measurements on anodes and cathodes can be made simultaneously.

Tests have been done with a ^{90}Sr source collimated to 5 mm in diameter by a plexiglass block and then to 1 mm^2 by coincidence of two small staggered scintillation counters S_1 and S_2 (see Fig. 1).

Signals from cathodes, anodes and scintillators are amplified and shaped through standard NIM[4] modules and analyzed via a CAMAC[5] data acquisition system connected to a NORD 10 computer.

Efficiencies, signal amplitude spectra and jitters are obtained with this set up.

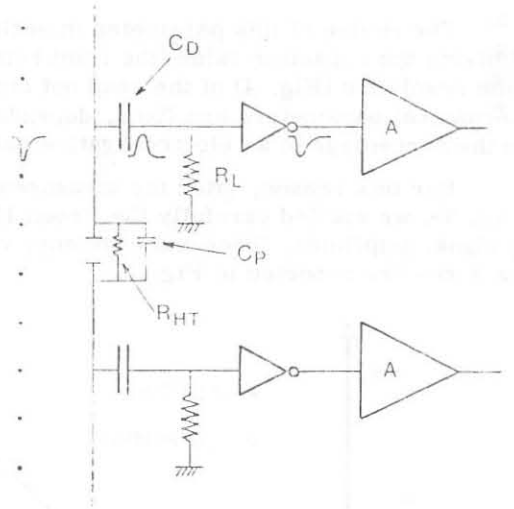

FIG. 3 - Equivalent circuit of the cathodes and their preamplifiers.

3. - EXPERIMENTAL RESULTS.

The first approach was to determine the high voltage capacitor value.

The signal coming from a cathode mesh was filtered through capacitors ranging from 10 to 300 pF (with $R_{LOAD} = 50\ \Omega$). The pulse amplitude and jitters are shown in Fig. 4. Values between 15 and 50 pF were chosen for the prototype chamber, as they give good efficiencies and limit the cross-talk between neighbouring squares.

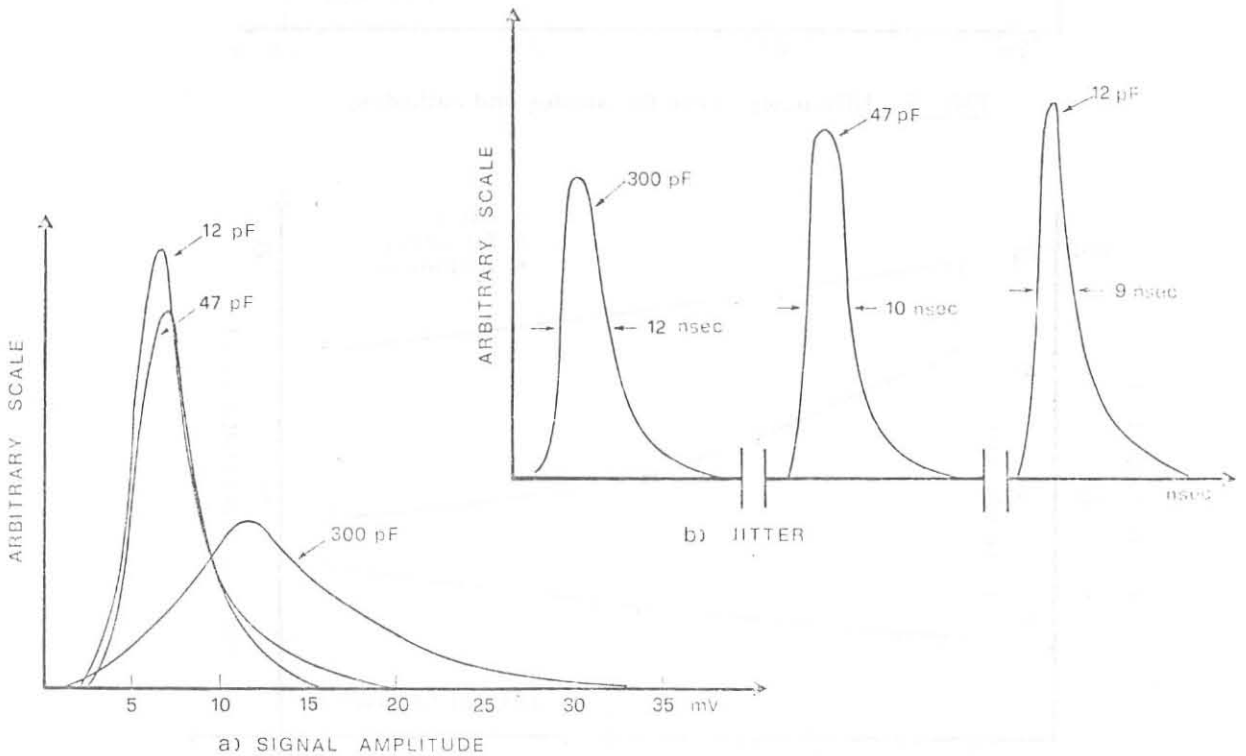

FIG. 4 - Variation of pulse amplitude (a) and jitter (b) of a single cathode with the decoupling capacitor value.

The choice of this parameter in such a chamber is very important. We simply stress that minimizing the capacitor value (the limit being given by the readibility of the signal) allows a better time resolution (Fig. 4) of the read out chain. The intrinsic time resolution of a MWPC, once the mechanical parameters are fixed, depends on the gas mixture used for filling it and, in particular, on the percentage of an electronegative gas like the Freon 13B1[6].

For this reason, after the measurement of the efficiency curve for both wires and squares (Fig. 5), we studied carefully the Freon 13B1 percentage dependence of the chamber, looking into signal amplitude, jitter and efficiency variation for the cathodes (Fig. 6). The same data for the wires are reported in Fig. 7.

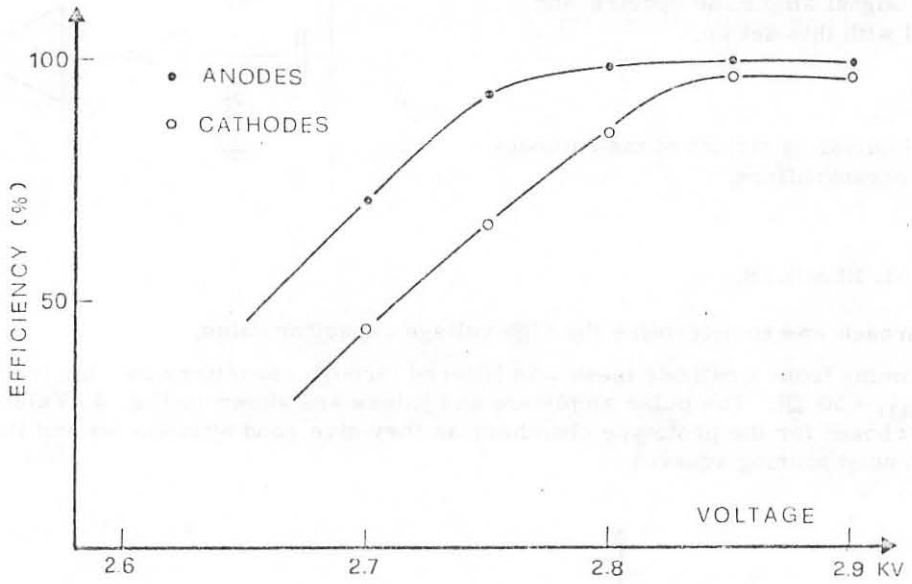

FIG. 5 - Efficiency curve for anodes and cathodes.

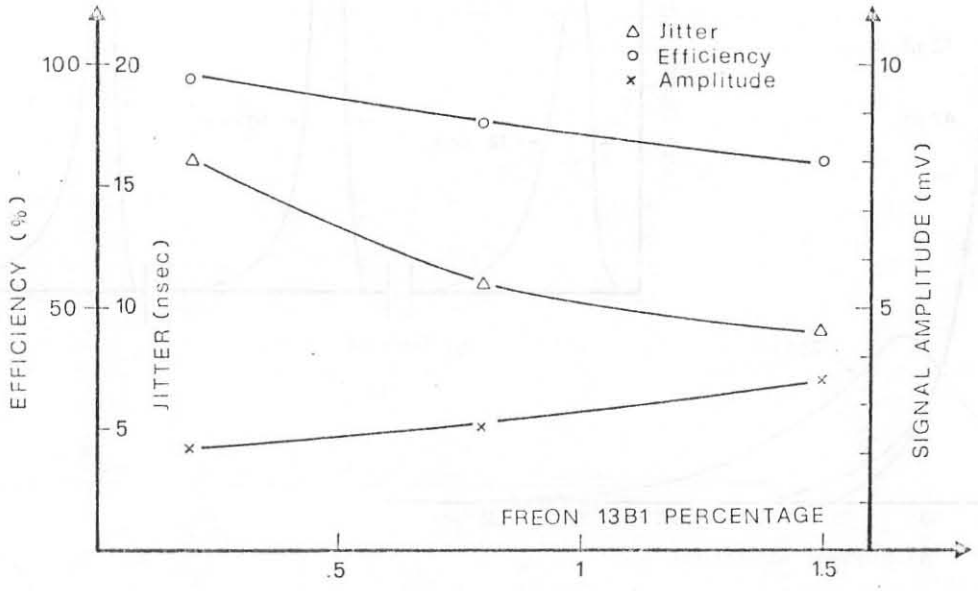

FIG. 6 - Cathode characteristic variation with Freon 13B1 percentage.

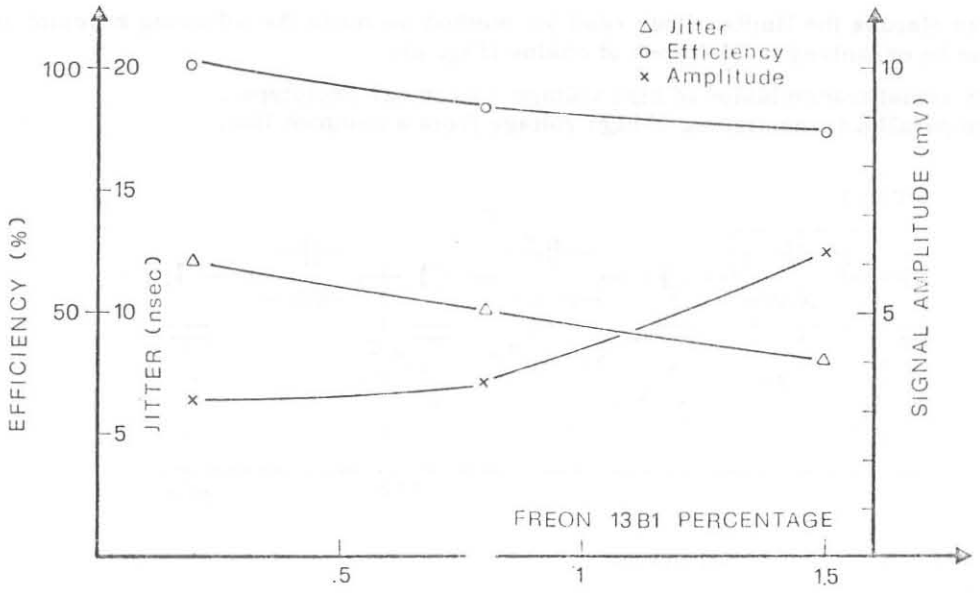

FIG. 7 - Anode characteristic variation with Freon 13B1 percentage.

Finally the cross-talk between neighbouring squares is studied, centering the β-source on a cathode segment and looking at the signals coming from the others. The result of this test is illustrated in Table II.

TABLE II

% Freon \ Chess A ε ‰ when source is on chess :	B	C	D
0.2	17	4	0
0.8	13	8	0
1.5	22	8	4

4. - COMMENTS ON EXPERIMENTAL RESULTS AND LIMITS OF THE METHOD.

Our detection system has the following parameters (see Fig. 3) :

$R_{H-T} = 100\ K\Omega$,

$C_P = 5\ pF$,

$15 \leq C_D \leq 50\ pF$,

$R_{LOAD} = 50\ \Omega$,

Number of cathodes = 4 .

In order to discuss the limits of our read out method we made the following schematization. The chesses can be organized in two types of chains (Fig. 8):

A) with serial transmission of high voltage - as in our prototype ,
B) with parallel transmission of high voltage from a common line.

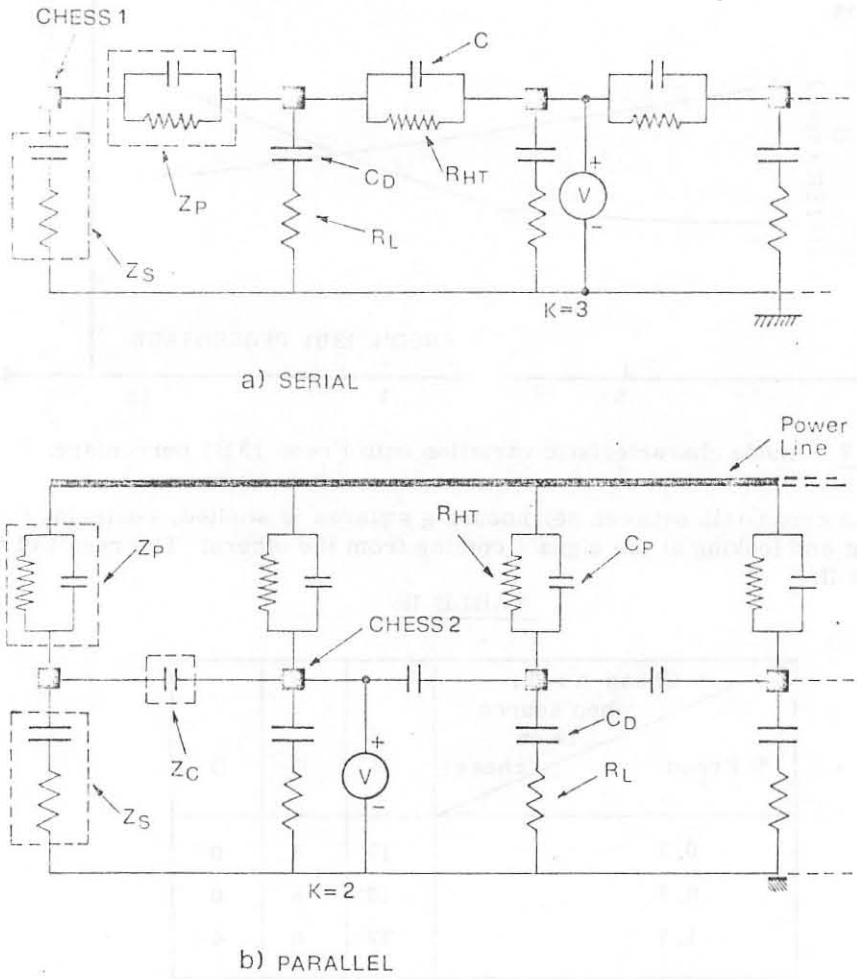

FIG. 8 - Electronic schemes of the two fundamental types of cathode chains: a) serial, b) parallel.

The aim of the analysis we are reporting was to find the values of the relevant parameters listed above for which the signal to cross-talk ratio was better.

The possible cause of cross-talk between neighbouring elements is the RC (or simply the C) interconnecting them. The first approach was to check the validity of our method with our experimental data, so:

a) We fitted the induced pulse with the following curve

$$V(t) = \begin{cases} 0 & t < 0 \\ (V_1/t_1)\,t & 0 \leq t < t_1 \\ A\,t^2 + B\,t + C & t_1 \leq t < t_1 \\ V_1 \exp\left(-\ln 2 \dfrac{t - t_3}{t_4 - t_3}\right) & t_3 \leq t \leq t_5 \end{cases}$$

$$A = -\frac{V_2 - V_1}{(T_3 - T_2)(T_2 - T_1)} \qquad B = -(T_3 + T_1)A ,$$

$$C = V_1 - AT_1^2 - BT_1 , \qquad t_1 = 20 \text{ nsec} ,$$

$$t_2 = 60 \text{ nsec} , \qquad t_3 = 80 \text{ nsec} ,$$

$$t_4 = 400 \text{ nsec} , \qquad t_5 = 980 \text{ nsec} ,$$

$$V_1 = 120 \text{ mV} , \qquad V_2 = 150 \text{ mV}$$

b) We found the Fourier power spectrum (FPS) of this pulse.

c) We found the transfer function (T) for signals picked-up on neighbouring elements to the hit one in chains A and B and when the coupling is simply capacitive (chain C).

d) We made the convolutions between the power spectrum (Fig. 9) and the transfer functions and found the results shown in Fig. 10.

Putting together the information contained in this figure and in Fig. 4a we have good agreement with results shown in Table II. Having proved the applicability of our analysis approach we tried to find the optimum values of parameters for all the configurations of chesses.

In order to perform a more general analysis we restricted the range of variation of some of the parameters. It is obvious (Fig. 9) that the cross-talk will be minimized by reducing as much as possible the value C_p. A reasonable limit for C_p can be deduced from reference (3a) where two conducting deposits of 8 μm thickness spaced by 2 mm (i.e. the maximum value for avoiding efficiency losses) over a lenght 20 cm have ~ 0.5 pF of mutual capacitance. We took this value as the limit for C_p; what will be described hereafter is obviously overstimated for chesses less than 20×20 cm^2 using current technology.

A lower limit for R_{HT} is due to the need of inhibiting the resistive way of cross-talk. A reasonable value, as confirmed by the following calculation, is ~ 100 K.

On the other hand the number of chesses connected in series gives an upper limit to R_{HT}, because of the voltage drop when a reasonable flux of particles crosses the chamber. We have

$$N < \frac{L}{R_{HT} \Sigma_i I_i}$$

with

N = number of chesses connected in series ,
L = length of the efficiency plateau ,
I_i = current drawn by the i-th chess of the chain .

For this reason we restricted ourselves to consider values of R_{HT} lower than 5 MΩ .

The C_D range can lie between 10 and 100 pF for time resolution reasons already mentioned and because the fast charge amplifiers which can be used with this device[7] match well with these capacitor values.

The R_L values can vary between 50 Ω of standard NIM[4] modules and a few KΩ of fast charge preamplifiers.

If energy measurement (i.e. better linearity between input charge and output voltage) is required the upper limit of R_L has be to increased.

We would now repeat the same convolutions we did for our test cathode plane using the parameter values in the range we defined before. We limited ourselves to analyze two-element chains of various types (A, B and C) because obviously the maximum cross-talk is between neighbouring

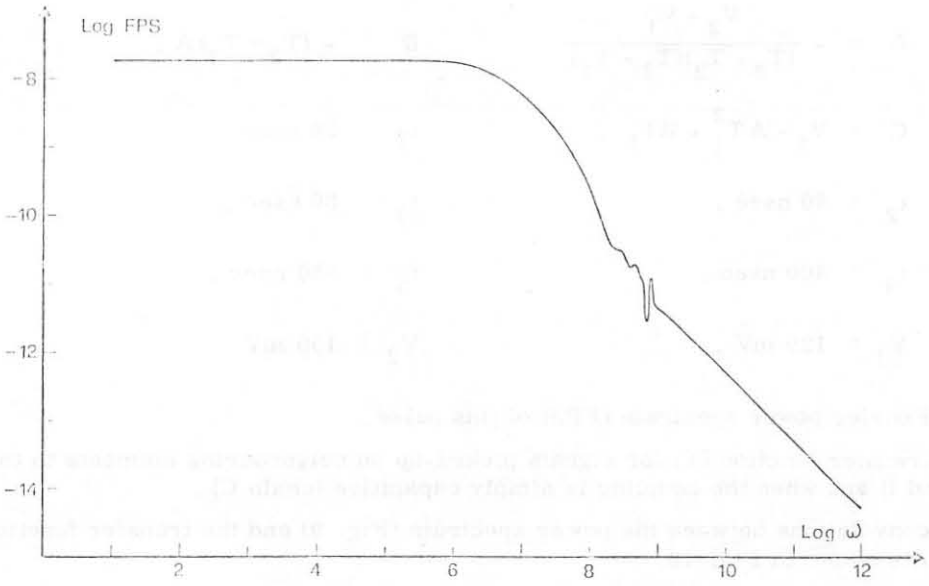

FIG. 9 - Power spectrum of a typical pulse induced on cathodes.

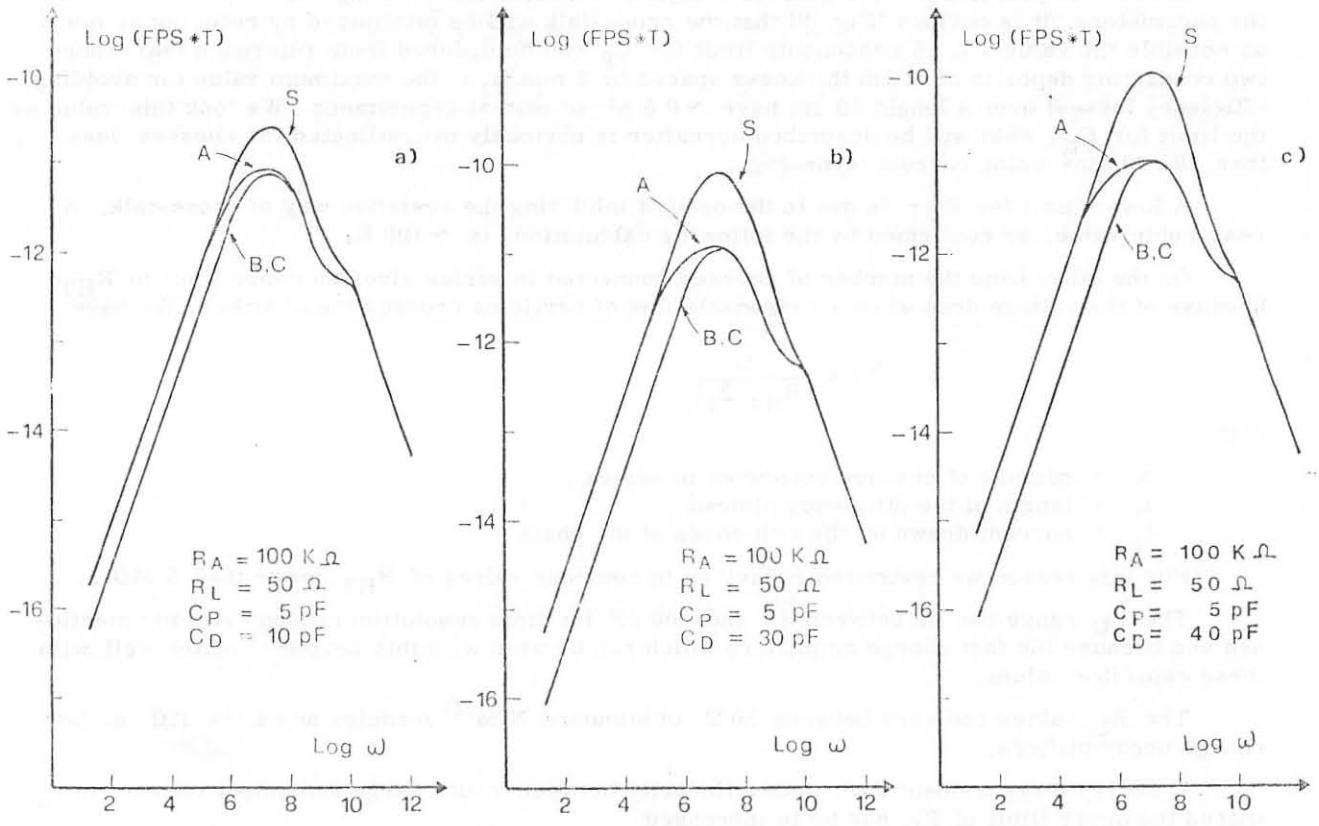

FIG. 10 - Convolutions between FPS and T curves with values of relevant parameters matching our experimental set-up. We define: Curve S: read-out on the hit cathode; Curve A: read-out on a cathode neighbouring to the hit one, chain A; Curve B: the same for chain B; Curve C: the same for chain C.

chesses. In Fig. 11 the convolution is shown for three different C_D values.

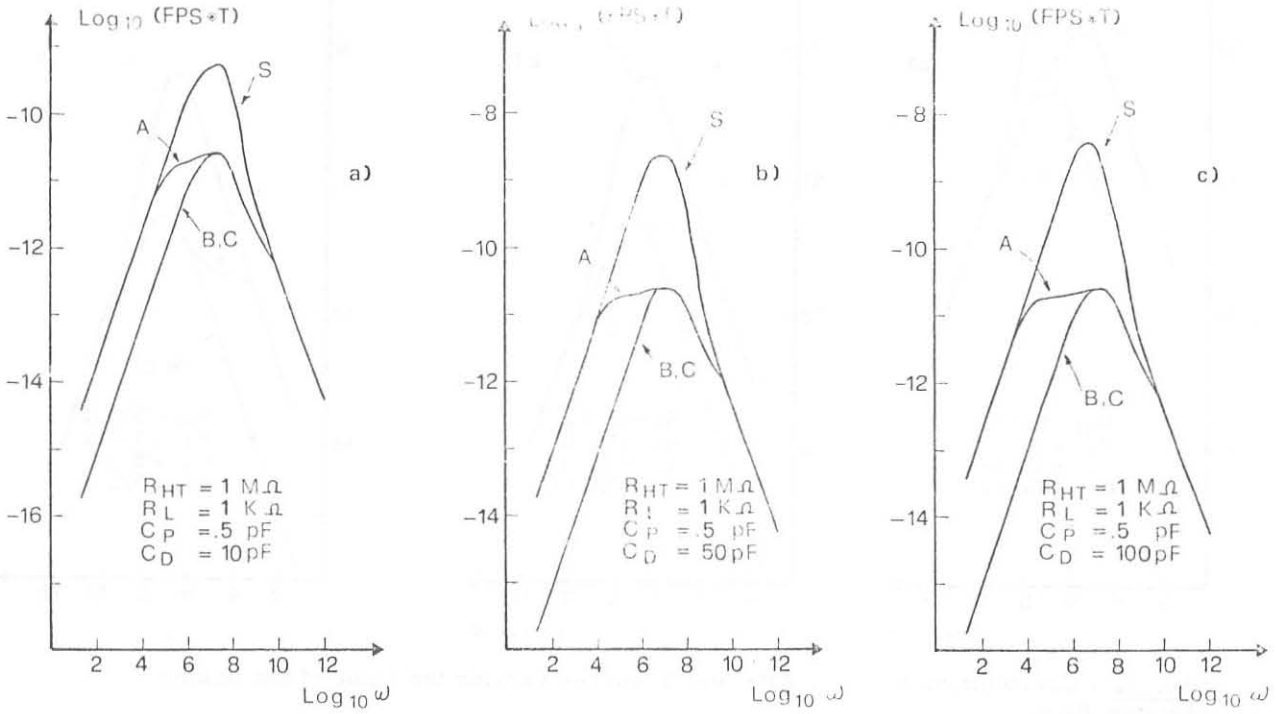

FIG. 11 - Convolutions between FPS and T curves varying the value of the decoupling capacitor C_D.

The relative importance of this parameter doesn't change with the other parameters ranging in their chosen intervals, so we fixed C_D at 100 pF.

In Fig. 12 the convolution is shown varying the linking resistor R_{HT} while in Fig. 13 we present the dependence on R_L. From the previous results we see that we can adopt parameter values in such a way as to match widely different experimental situations all with a good signal to cross-talk ratio.

Better comparisons between different chess organizations can be done solving linear systems equations describing chains A, B and C (see Fig. 8).

Chain A

For j = 1 to N

row j : $(1 - \delta_{j,K} - \delta_{j,K+1})\left[-(1 - \delta_{j,1})I_{j-1}Z_s + I_j(2Z_s + Z_p) - I_{j+1}Z_s(1 - \delta_{j,N})\right] +$

$+ \delta_{j,K}\left[-(1 - \delta_{j,1})I_{j-1}Z_s + I_jZ_s + V\right] + \delta_{j,K+1}\left[I_j(Z_s + Z_p) - (1 - \delta_{j,N})I_{j+1}Z_s - V\right] = 0$

Chain B

For j = 1 to K

row 2j - 1 : $(1 - \delta_{j,K})\left[-(1 - \delta_{j,1})I_{2j-3}Z_s + I_{2j-1}(2Z_s + Z_c) - I_{2j}Z_c - I_{2j+1}Z_s\right] +$

$+ \delta_{j,K}\left[-(1 - \delta_{j,1})I_{2j-3}Z_s + I_{2j-1}Z_s + V\right] = 0$

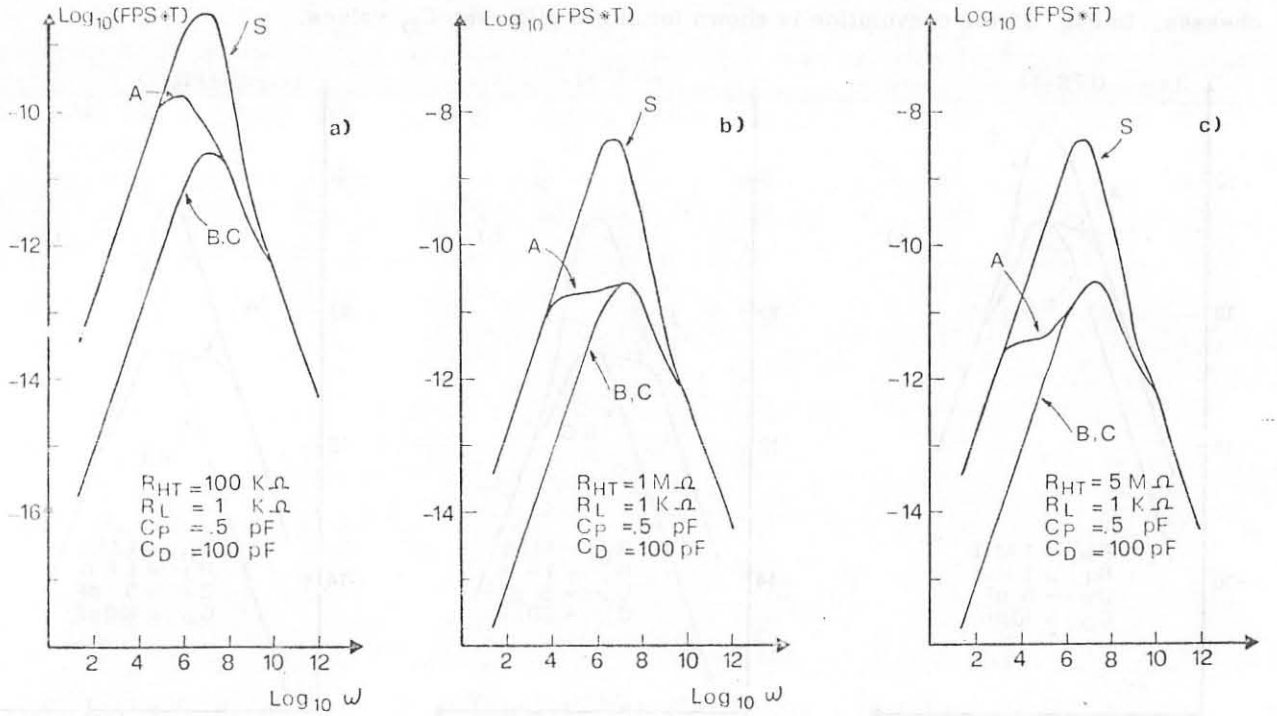

FIG. 12 - Convolutions between FPS and T curves varying the value of the linking resistor R_{HT}.

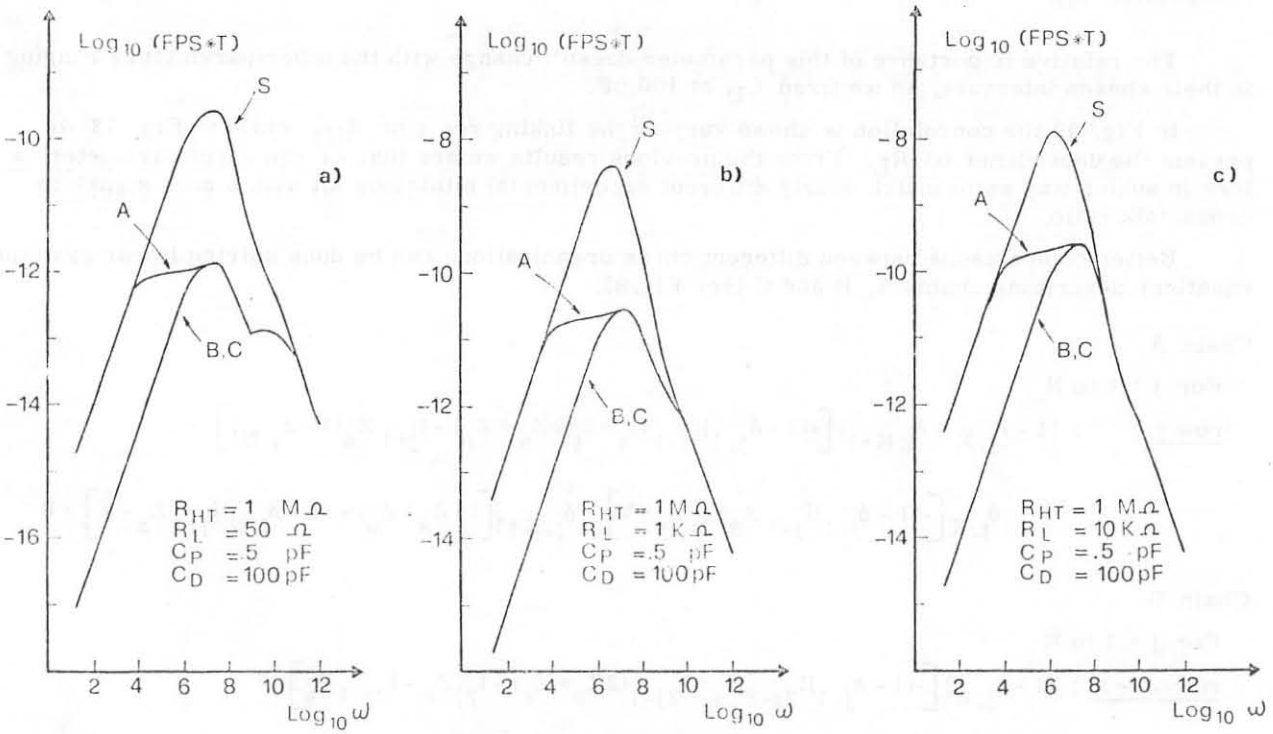

FIG. 13 - Convolutions between FPS and T curves varying the value of the load resistor R_L.

$$\underline{\text{row } 2j} \quad : (1-\delta_{j,K})\Big[-(1-\delta_{j,1})I_{2j-2}Z_p - I_{2j-1}Z_c + I_{2j}(2Z_p+Z_c) -$$

$$- (1-\delta_{j,K-1})I_{2j+2}Z_p - \delta_{j,K-1}(1-\delta_{j,N-1})I_{2j+3}Z_p\Big] = 0$$

For $j = K$ to $N-1$

$$\underline{\text{row } 2j} \quad : (1-\delta_{j,K})\Big[-I_{2j-2}Z_s - I_{2j+1}Z_c + I_{2j}(2Z_s+Z_c) - (1-\delta_{j,N-1})I_{2j+2}Z_s\Big] +$$

$$+(1-\delta_{K,N})\,\delta_{j,K}\Big[I_{2j}(Z_s+Z_c) - I_{2j+1}Z_c - (1-\delta_{j,N})I_{2j+2}Z_s - V\Big] = 0$$

$$\underline{\text{row } 2j+1} \quad : (1-\delta_{K,N})\Big[-(1-\delta_{K,1})\delta_{j,K}I_{2j-2}Z_p - (1-\delta_{j,K})I_{2j-1}Z_p - I_{2j}Z_c +$$

$$+ I_{2j+1}(2Z_p+Z_c) - (1-\delta_{j,N-1})I_{2j+3}Z_p\Big] = 0$$

Chain C

The same as chain A with $R_{HT} = 0$

With Z_s, Z_p, Z_c as in Fig. 8

k = i means: event on chess i

V is a sinusoidal wave of frequency ω .

Doing so we get the effective voltage V_s on each chess

$$V_s = |I|\, R_L \cos(\omega t - \text{arctg}(\text{im}I/\text{re}I)$$

where:

I is the current, due to the primary pulse, drawn by the chess,

t is the time at which we pick-up the signal (about 40 nsec from the start of the pulse).

This allows the study of more complicated configurations and, in particular, of the cross-talk propagation to distant chesses. We solved these systems with a computer program varying the previous relevant parameters and moreover ω, N_A, N_B, N_C (N_A = number of chesses of chain A, etc.). Considering that the rise time of the primary pulse is of the order of 20 nsec, that we are mainly interested in the high frequency part of the signal because we want good time resolution, and taking into account the shape of the curves SPS*T, we can restrict ourselves to frequencies ranging from the maxima of S curves (about 10^7 Hz to 10^9 Hz).

In Fig. 14 we show the ω-dependence of the effective voltage on various chesses of different chain types. The fixed parameters have been chosen considering the results of the convolutions already presented.

In Figg. 15, 16, 17, 18 the dependence on R_{HT}, R_L, C_D, C_p is shown.

We can summarize the results of our calculations in the following way:

a) Our experimental apparatus was not optimized. A factor of ten in the signal to noise ratio can be gained, mainly reducing C_D.

b) C_D and R_{HT} are the more critical parameters. In order to inhibit the cross-talk the first one has to be minimized, the limit being the deposition technique one adopts for the chesses; the second one has to be maximized, the limit being the particles flux through the chamber.

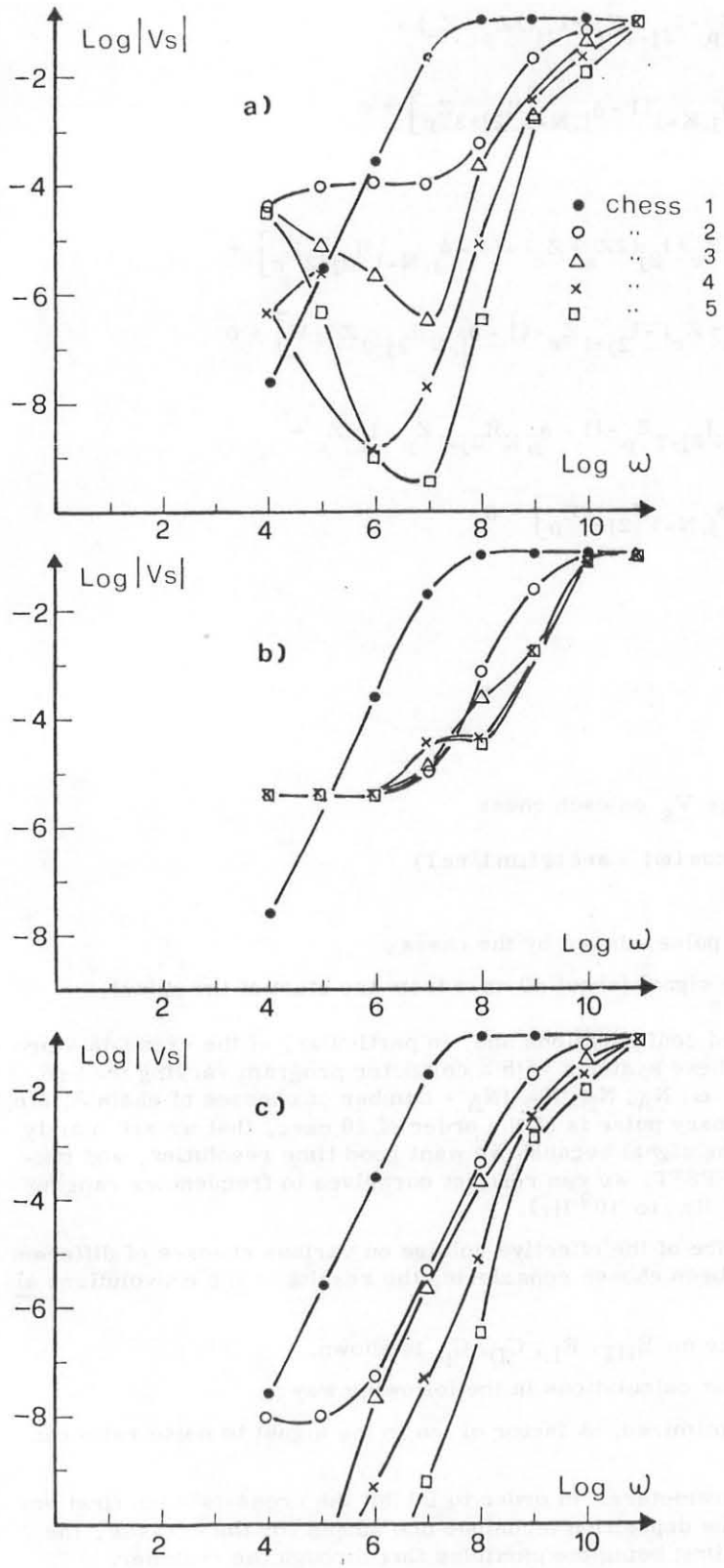

a) Chain A

R_{HT} = 1 MΩ ,

R_L = 1 KΩ ,

C_p = 0.5 pF ,

C_D = 50 pF ,

N_A = 5 .

b) Chain B

R_{HT} = 5 MΩ ,

R_L = 1 KΩ ,

C_p = 0.5 pF ,

C_D = 50 pF ,

N_B = 5 .

c) Chain C

R_{HT} = 10 GΩ ,

R_L = 1 KΩ ,

C_p = 0.5 pF ,

C_D = 50 pF ,

N_C = 5 .

FIG. 14 - Frequency dependence of the effective voltage V_s on different chesses.

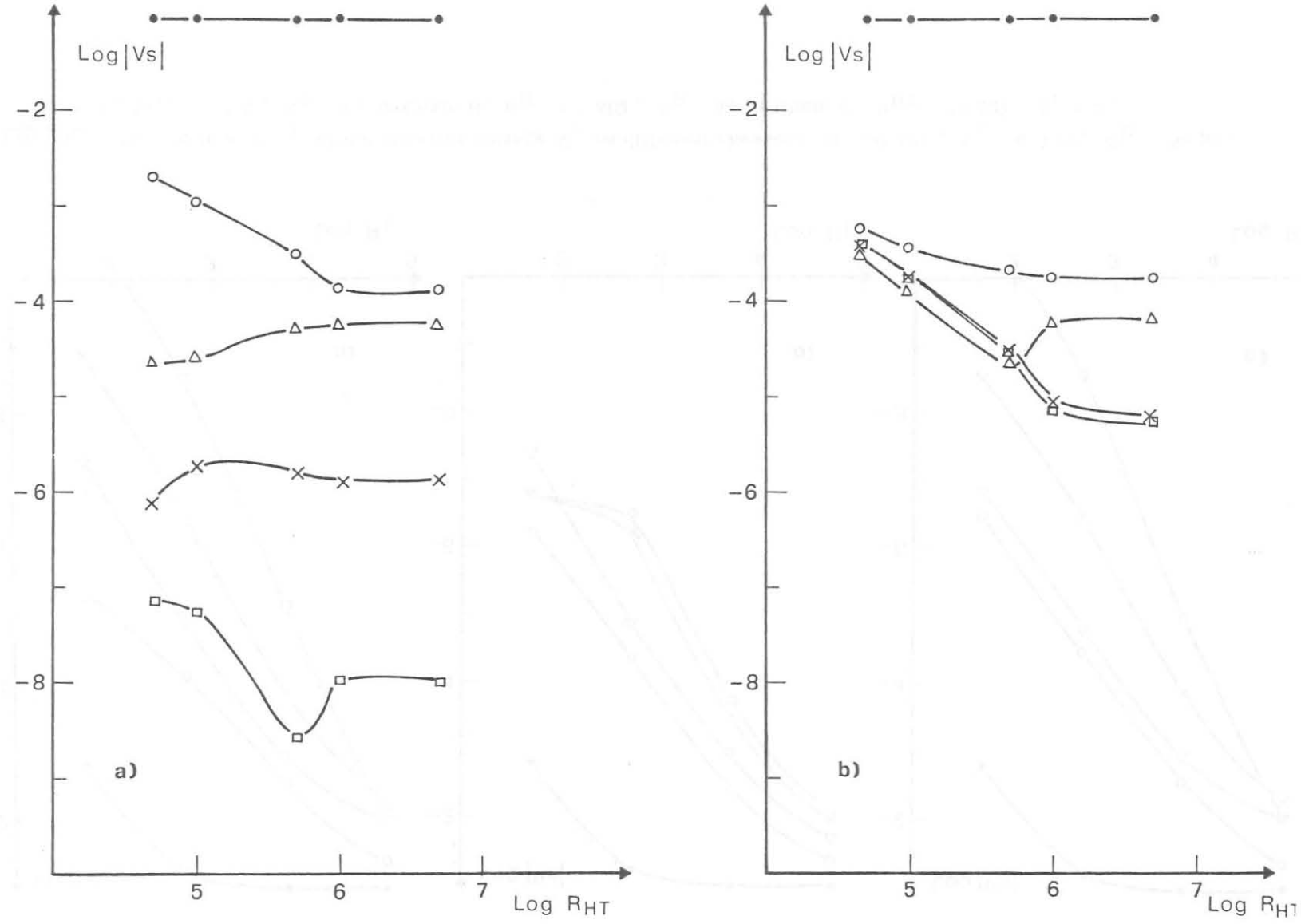

FIG. 15 - Dependence on R_{HT} of the effective voltage V_s on different chesses : ω = 50 MHz, R_L = 1 KΩ , C_p = 0.5 pF, C_D = 50 pF . a) Chain A : N_A = 5 ; b) Chain B : N_B = 5.

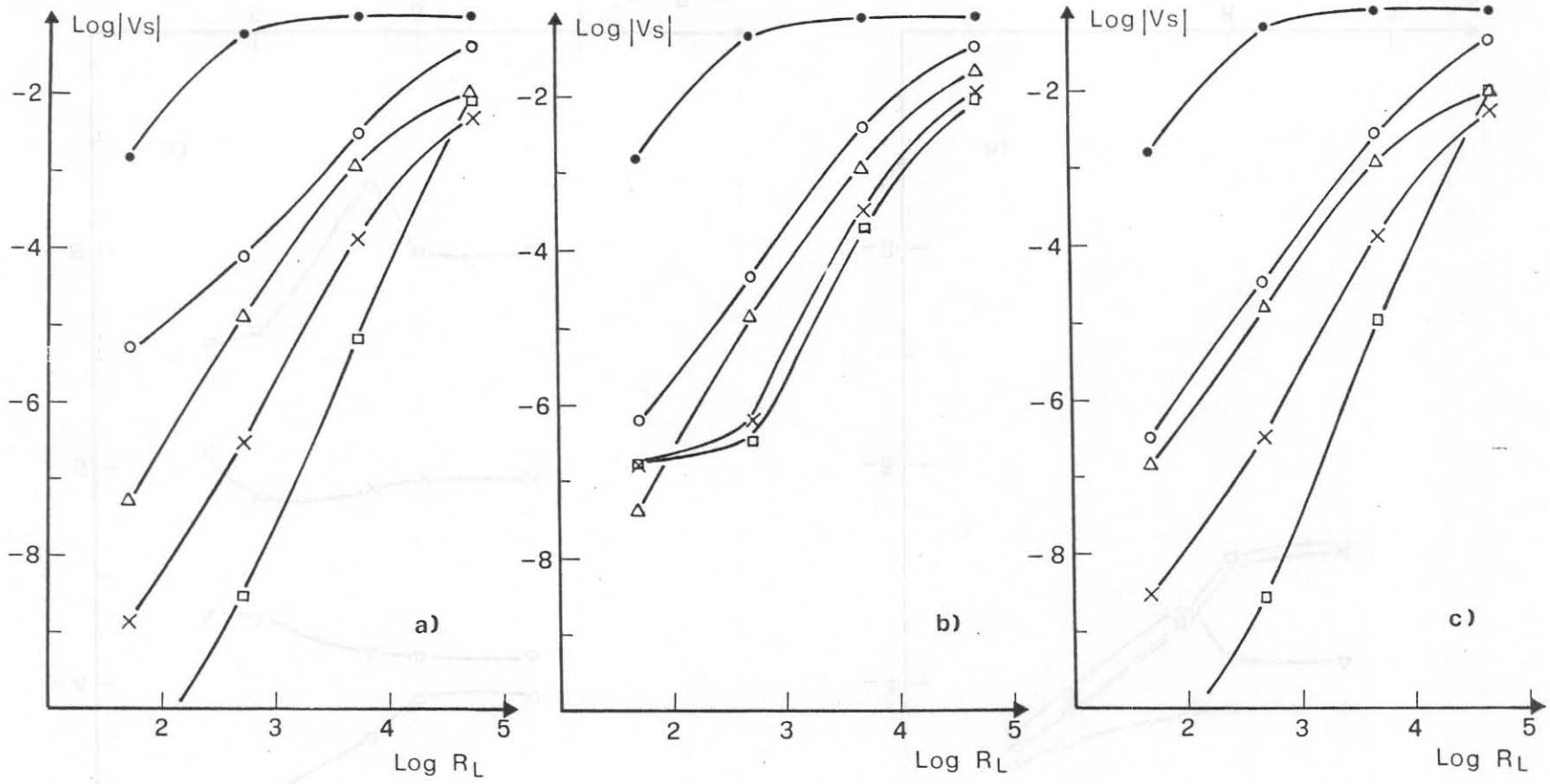

FIG. 16 - Dependence on R_L of the effective voltage V_s on different chesses : ω = 50 MHz, C_p = 0.5 pF, C_D = 50 pF.
a) Chain A : R_{HT} = 1 MΩ, N_A = 5 ; b) Chain B : R_{HT} = 5 MΩ, N_B = 5 ; c) Chain C : R_{HT} = 10 GΩ, N_C = 5.

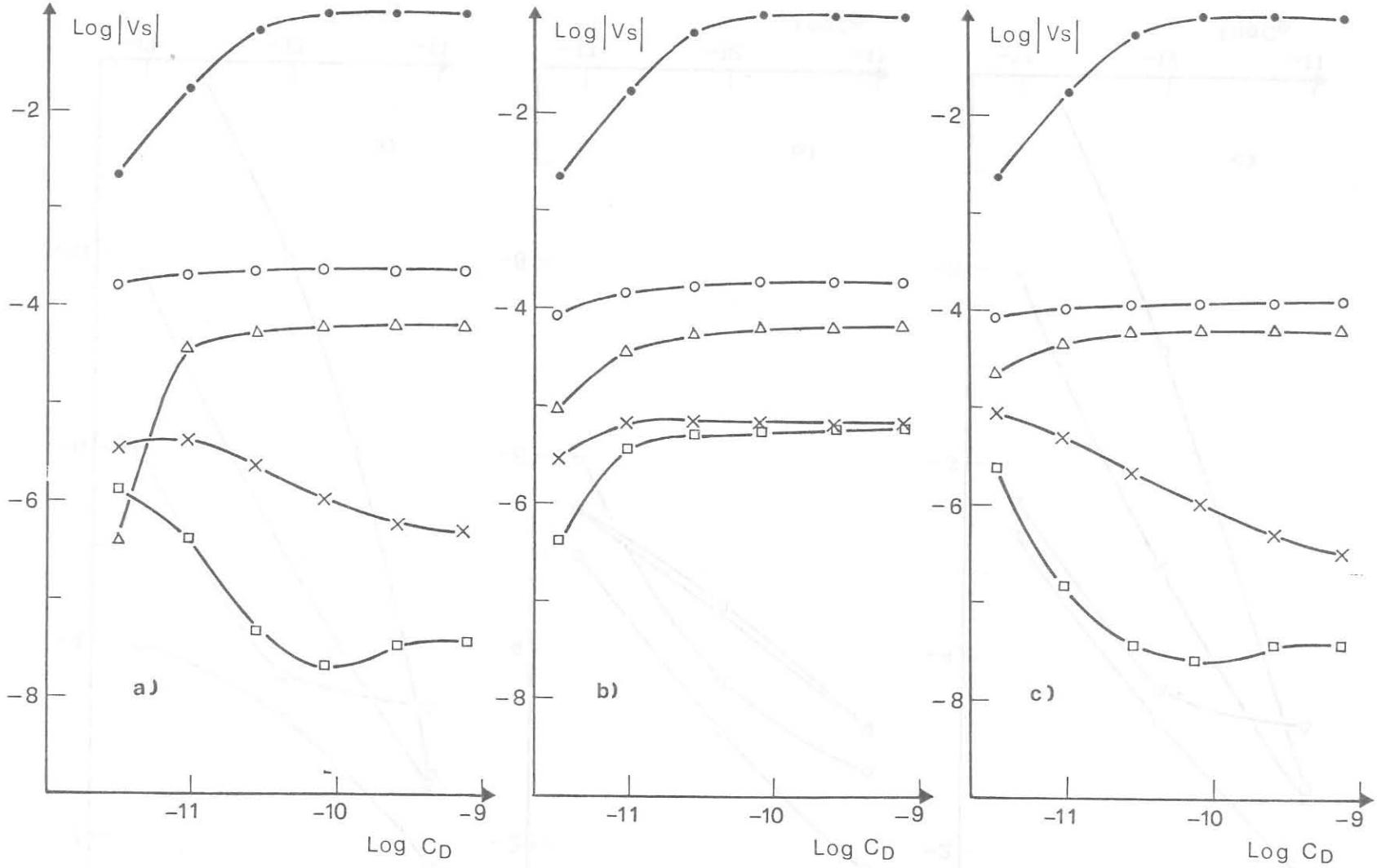

FIG. 17 - Dependence on C_D of the effective voltage V_s on different chesses : ω = 50 MHz, C_p = 0.5 pF, R_L = 1 KΩ , a) Chain A : R_{HT} = 1 MΩ , N_A = 5 ; b) Chain B : R_{HT} = 5 MΩ , N_B = 5 ; c) Chain C : R_{HT} = 10 GΩ , N_C = 5.

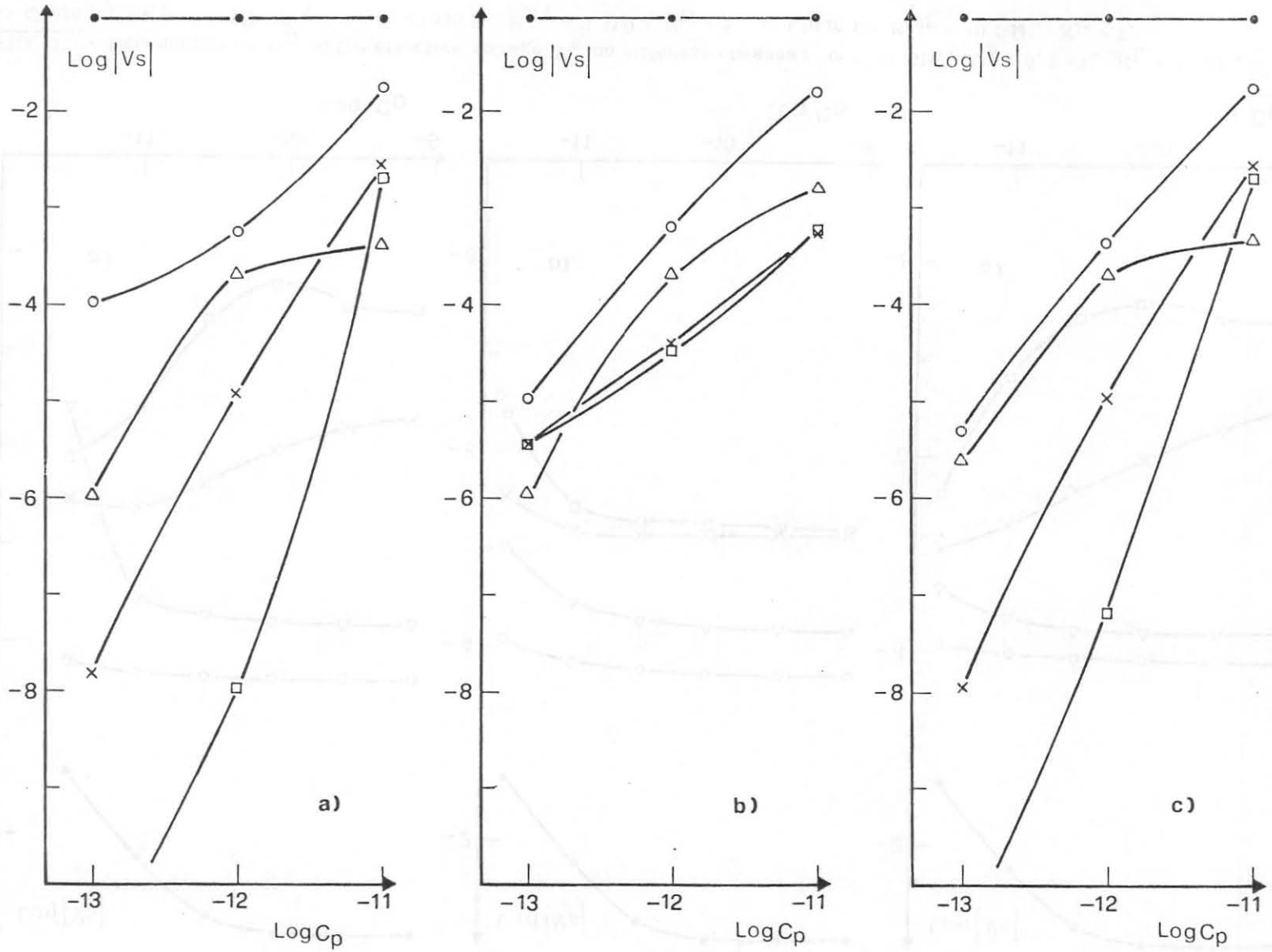

FIG. 18 - Dependence on C_p of the effective voltage V_s on different chesses : ω = 50 MHz, R_L = 1 KΩ , C_D = 50 pF .
a) Chain A : R_{HT} = 1 MΩ , N_A = 5 ; b) Chain B : R_{HT} = 5 MΩ , N_B = 5 ; c) Chain C : R_{HT} = 10 GΩ , N_C = 5.

c) Parallel and serial configuration of chesses are roughly equivalent. Putting together both these configurations on a single high voltage plane allows a full coverture of the sensitive zone of a chamber with a high number of independent elements

5. - CONCLUSIONS.

Test performed on a multiwire proportional chamber with anode and cathode read-out and calculations on a new method used for picking-up signals from the cathodes show that one can build up complex configurations of cathodes without efficiency losses in the whole chamber. The minimum dimension of cathodic elements is ~ 1 cm^2, because of the induced-signal spread[8], while the maximum dimension is limited by the cross-talk between neighbouring elements.

One such chamber with 64 cathodic elements is under test for being employed as a hodoscope in the WA7 experiment at CERN SPS.

The use of the cathode information makes the point finding algorithm easier and quicker (in comparison with the present technique of redundant planes tilted at various angles)[9].

ACKNOWLEDGMENTS.

We are indebted to A. Buzzo for fruitful discussions and to G. Barisone and P. Poggi for their skilful technical support.

REFERENCES.

(1) - J. L. Lacy and R. S. Lindsay, Nuclear Instr. and Meth. 119, 483 (1974); A. Derevschikov, I. Golutvin and L. Rossi, Report INFN-GE AEB 103 (1974).
(2) - H. Foeth, R. Hammarström and C. Rubbia, Nuclear Instr. and Meth. 109, 521 (1973).
(3) - M. Davier, M. G. D. Gilchriese and D. W. G. S. Leith, Nuclear Instr. and Meth. 131, 229 (1975); J. N. Marx and D. R. Nygren, Phys. Today, Oct. (1978), p. 46.
(4) - TID, 20893 (Rev. 4), U. S. Atomic Energy Commission (July 1974).
(5) - ESONE Commitee, EUR 4100 e (Rev. 2) (1972).
(6) - G. Grundberg, L. Lohen and L. Mathieu, Nuclear Instr. and Meth. 78, 102 (1970).
(7) - J. C. Santiard, Report CERN/EP/JCS/ef (1976).
(8) - G. Fisher and J. Plch, Nuclear Instr. and Meth. 100, 515 (1972).
(9) - S. Benso and L. Rossi, paper in preparation.